2014

Searching for Pulsars Using Image Pattern Recognition

W. W. Zhu

A. Berndsen

E. C. Madsen

M. Tan

Fronefield Crawford
Haverford College, fcrawford@haverford.edu

Repository Citation

"Searching for Pulsars Using Image Pattern Recognition" W. W. Zhu, A. Berndsen, E. C. Madsen, M. Tan, I. H. Stairs, A. Brazier, P. Lazarus, R. Lynch, P. Scholz, K. Stovall, S. M. Ransom, S. Banaszak, C. M. Biwer, S. Cohen, L. P. Dartez, J. Flanigan, G. Lunsford, J. G. Matinez, A. Mata, M. Rohr, A. Walker, B. Allen, N. D. R. Bhat, S. Bogdanov, F. Camilo, S. Chatterjee, J. M. Cordes, F. Crawford, J. S. Deneva, G. Desvignes, R. D. Ferdman, J. W. T. Hessels, F. A. Jenet, D. Kaplan, V. M. Kaspi, B. Knispel, K. J. Lee, J. van Leeuwen, A. G. Lyne, M. A. McLaughlin, L. G. Spitler, and A. Venkataraman, Astrophysical Journal, 781, 117 (2014).

The Astrophysical Journal, 787:137 (10pp), 2014 June 1 doi:10.1088/0004-637X/787/2/137

ARECIBO PULSAR SURVEY USING ALFA. III. PRECURSOR SURVEY AND POPULATION SYNTHESIS

J. K. Swiggum[1], D. R. Lorimer[1], M. A. McLaughlin[1], S. D. Bates[1,2], D. J. Champion[3], S. M. Ransom[4], P. Lazarus[3], A. Brazier[5], J. W. T. Hessels[6,7], D. J. Nice[8], J. Ellis[9], T. R. Senty[1], B. Allen[9,10,11], N. D. R. Bhat[12], S. Bogdanov[13], F. Camilo[13,14], S. Chatterjee[5], J. M. Cordes[5], F. Crawford[15], J. S. Deneva[14], P. C. C. Freire[3], F. A. Jenet[16], C. Karako–Argaman[17], V. M. Kaspi[17], B. Knispel[10,11], K. J. Lee[3,18], J. van Leeuwen[6,7], R. Lynch[17], A. G. Lyne[2], P. Scholz[17], X. Siemens[9], I. H. Stairs[19], B. W. Stappers[2], K. Stovall[20], A. Venkataraman[14], and W. W. Zhu[19]
[1] Department of Physics and Astronomy, West Virginia University, Morgantown, WV 26506, USA
[2] Jodrell Bank Centre for Astrophysics, School of Physics and Astronomy, University of Manchester, Manchester, M13 9PL, UK
[3] Max-Planck-Institut für Radioastronomie, D-53121 Bonn, Germany
[4] NRAO, Charlottesville, VA 22903, USA
[5] Astronomy Department, Cornell University, Ithaca, NY 14853, USA
[6] ASTRON, Netherlands Institute for Radio Astronomy, Postbus 2, 7990 AA, Dwingeloo, The Netherlands
[7] Astronomical Institute "Anton Pannekoek," University of Amsterdam, Science Park 904, 1098 XH Amsterdam, The Netherlands
[8] Department of Physics, Lafayette College, Easton, PA 18042, USA
[9] Physics Department, University of Wisconsin – Milwaukee, Milwaukee WI 53211, USA
[10] Leibniz Universität Hannover, D-30167 Hannover, Germany
[11] Max-Planck-Institut für Gravitationsphysik, D-30167 Hannover, Germany
[12] Center for Astrophysics and Supercomputing, Swinburne University, Hawthorn, Victoria 3122, Australia
[13] Columbia Astrophysics Laboratory, Columbia University, New York, NY 10027, USA
[14] Arecibo Observatory, HC3 Box 53995, Arecibo, PR 00612, USA
[15] Department of Physics and Astronomy, Franklin and Marshall College, Lancaster, PA 17604-3003, USA
[16] Center for Gravitational Wave Astronomy, University of Texas at Brownsville, TX 78520, USA
[17] Department of Physics, McGill University, Montreal, QC H3A 2T8, Canada
[18] Kavli Institute for Radio Astronomy, Peking University, Beijing 100871, China
[19] Department of Physics and Astronomy, University of British Columbia, 6224 Agricultural Road Vancouver, BC V6T 1Z1, Canada
[20] Department of Physics and Astronomy, University of New Mexico, NM, 87131, USA
Received 2013 October 23; accepted 2014 April 20; published 2014 May 13

ABSTRACT

The Pulsar Arecibo L-band Feed Array (PALFA) Survey uses the ALFA 7-beam receiver to search both inner and outer Galactic sectors visible from Arecibo ($32^\circ \lesssim \ell \lesssim 77^\circ$ and $168^\circ \lesssim \ell \lesssim 214^\circ$) close to the Galactic plane ($|b| \lesssim 5^\circ$) for pulsars. The PALFA survey is sensitive to sources fainter and more distant than have previously been seen because of Arecibo's unrivaled sensitivity. In this paper we detail a precursor survey of this region with PALFA, which observed a subset of the full region (slightly more restrictive in ℓ and $|b| \lesssim 1^\circ$) and detected 45 pulsars. Detections included 1 known millisecond pulsar and 11 previously unknown, long-period pulsars. In the surveyed part of the sky that overlaps with the Parkes Multibeam Pulsar Survey ($36^\circ \lesssim \ell \lesssim 50^\circ$), PALFA is probing deeper than the Parkes survey, with four discoveries in this region. For both Galactic millisecond and normal pulsar populations, we compare the survey's detections with simulations to model these populations and, in particular, to estimate the number of observable pulsars in the Galaxy. We place 95% confidence intervals of 82,000 to 143,000 on the number of detectable normal pulsars and 9000 to 100,000 on the number of detectable millisecond pulsars in the Galactic disk. These are consistent with previous estimates. Given the most likely population size in each case (107,000 and 15,000 for normal and millisecond pulsars, respectively), we extend survey detection simulations to predict that, when complete, the full PALFA survey should have detected 1000^{+330}_{-230} normal pulsars and 30^{+200}_{-20} millisecond pulsars. Identical estimation techniques predict that 490^{+160}_{-115} normal pulsars and 12^{+70}_{-5} millisecond pulsars would be detected by the beginning of 2014; at the time, the PALFA survey had detected 283 normal pulsars and 31 millisecond pulsars, respectively. We attribute the deficiency in normal pulsar detections predominantly to the radio frequency interference environment at Arecibo and perhaps also scintillation—both effects that are currently not accounted for in population simulation models.

Key words: methods: statistical – pulsars: general – surveys

1. INTRODUCTION

Our current knowledge of the non-recycled (hereafter *normal*) pulsar and millisecond pulsar (MSP) Galactic populations[21]—their spatial, period, and luminosity distributions—primarily comes from the results of the Parkes Multibeam Pulsar Survey (PMPS; Manchester et al. 2001; Morris et al. 2002; Kramer et al. 2003; Hobbs et al. 2004; Faulkner et al. 2004; Lorimer et al. 2006). Analyses of these results have shown that the Galactic normal pulsar population is made up of 30,000 ± 1100 sources beaming toward Earth with luminosities above 0.1 mJy kpc^2; their radial density profile is best described by a gamma function and their distance from the Galactic plane, by an exponential function with a scale height of 0.33 kpc (Lorimer et al. 2006). A more physically realistic treatment of pulsar luminosities involves using a log-normal luminosity function, which is demonstrated from pulsar population syntheses (e.g., Faucher-Giguère & Kaspi 2006). The advantage of this

[21] Although a number of traits separate normal from millisecond pulsars, the most distinct is an MSP's short spin period, which is the result of angular momentum transferred by material from a binary companion. For the remainder of this paper, we use $P = 30$ ms and $B_{\rm surf} = 10^{10}$ G as period and surface magnetic field thresholds to differentiate between MSPs ($P < 30$ ms, $B_{\rm surf} < 10^{10}$ G) and normal pulsars ($P > 30$ ms, $B_{\rm surf} > 10^{10}$ G), although there are certainly exceptions to this simple separation. A complete list of currently known Galactic MSPs can be found at http://astro.phys.wvu.edu/GalacticMSPs

approach is that it allows predictions of the *total* normal pulsar population size—not just the number above a certain luminosity cutoff; Faucher-Giguère & Kaspi (2006) predict that there are 120,000 ± 20,000 detectable, normal pulsars in the Galaxy.

Since there are only ∼10% as many known MSPs as normal pulsars (Manchester et al. 2005), we do not have the same level of knowledge about recycled pulsars' population parameters. The High Time Resolution Universe (HTRU) Survey (Keith et al. 2010) has added more normal pulsar discoveries to the PMPS haul and many MSPs as well (e.g., Bates et al. 2011; Burgay et al. 2013; Morris et al. 2002; Hobbs et al. 2004; Mickaliger et al. 2012). Recent analysis of the intermediate latitude portion of HTRU MSP detections by Levin et al. (2013) uses a scale factor method (Vivekanand & Narayan 1981; Lorimer et al. 1993) and 50 detected MSPs to place a lower limit of 30,000 ± 7000 on the Galactic MSP population size (considering sources whose luminosities exceed 0.2 mJy kpc^2). The scale height of the MSP population is fairly well established to be 500 pc (Lorimer 2005; Cordes & Chernoff 1997), but the spatial, period and luminosity functions are currently less well understood. Although many models can be ruled out, plausible MSP populations with a variety of underlying distributions are consistent with the observed sample (Lorimer 2010).

Despite the fact that Arecibo's latitude does not permit observations close to Galactic center like those at Parkes, the unique combination of Arecibo's sensitivity, paired with the high spectral resolution of its back-ends, provides a much deeper view through the Galaxy's dispersive medium, which often smears out signals from distant sources. Although the PMPS and HTRU surveys have sampled much of the sky surrounding the Galactic center—an area of the sky with high pulsar density—and have discovered over 1000 pulsars, Pulsar Arecibo L-band Feed Array (PALFA) provides a glimpse of the population density at larger Galactic radii ($R > 5\,kpc$), which will help improve the spatial features of future pulsar population models. Arecibo's ability to reach competitive sensitivity limits with short integration times (one to five minutes) makes acceleration searches for binaries unnecessary for all but the most exotic systems. Finally, Arecibo's unrivaled sensitivity allows PALFA to probe the low-luminosity end of the Galactic pulsar population, leading to a better understanding of the underlying luminosity distribution.

With Arecibo's unique capabilities, PALFA has great potential to discover many normal pulsars as well as MSPs, thus improving our statistical picture of each population's characteristics. Given the number of discoveries by PMPS, it has historically been used to refine pulsar population modeling assumptions for normal pulsars. Recent efforts have been made to discover additional MSPs in archival PMPS data (Mickaliger et al. 2012) with motivation to improve MSP population models. With higher sensitivity to dispersed sources and MSPs, the PALFA survey's influence on normal and millisecond pulsar population studies will complement those of the PMPS and HTRU surveys. MSPs are essential for the direct detection of gravitational waves by pulsar timing array projects (e.g., Demorest et al. 2013). The best way to increase our sensitivity to the stochastic background is to add new MSPs to the array (Siemens et al. 2013).

In this paper, we present the detections and discoveries from the initial phase of the PALFA survey, hereafter referred to as the "precursor survey." In Section 2, we describe the PALFA precursor survey parameters and sky coverage and introduce two pipelines used to process the raw data. We present the 45 detections made by the precursor survey in Section 3 and include an evaluation of the survey's efficacy based on measured and theoretically calculated signal-to-noise (S/N) ratios. In Section 4 we discuss the portion of sky in the precursor survey that overlapped with the PMPS and show preliminary evidence that PALFA will indeed be probing more distant, fainter sources. Comparing population simulations to precursor survey detection statistics, we generate probability density functions (PDFs) for normal and millisecond pulsar populations in Section 5. These PDFs inform the predictions we make about the total number of pulsars (normal and MSP) we expect to have detected when the full PALFA survey is complete. We conclude in Section 6, stating the most probable normal and millisecond pulsar population sizes according to the precursor survey results.

2. SKY COVERAGE AND DATA ANALYSIS

The PALFA precursor survey covered portions of two Galactic sectors—an inner Galaxy region, $36^\circ \lesssim \ell \lesssim 75^\circ$, tiled with 865 pointings, and an outer Galaxy region, $170^\circ \lesssim \ell \lesssim 210^\circ$, covered by 919 pointings. All pointings were within one degree of the Galactic plane ($|b| < 1^\circ$) and had dwell times of 134 and 67 s for inner- and outer-Galaxy regions respectively. The precursor survey used the Arecibo L-band Feed Array (ALFA) 7-beam receiver in conjunction with the Wideband Arecibo Pulsar Processor (WAPP) back-end (Dowd et al. 2000), which was set up to record 256 channels covering a 100 MHz bandwidth, centered at 1.42 GHz, every 64 μs. Each ALFA pointing includes seven distinct beam positions in a hexagonal pattern. As PALFA continues, the sky coverage will increase slightly in Galactic longitude ($32^\circ \lesssim \ell \lesssim 77^\circ$ and $168^\circ \lesssim \ell \lesssim 214^\circ$) and will extend to Galactic latitude $\pm 5^\circ$. For the remainder of the paper, we will refer to this extended spatial coverage (accompanied by a three-fold increase in bandwidth) as the *full PALFA survey*. The precursor survey, optimized for maximum efficiency and sensitivity, used a "sparse sampling" technique described in detail in Cordes et al. (2006); gaps left by the precursor survey will be covered in multiple passes by the full PALFA survey. PMPS overlaps with the southernmost regions covered by Arecibo in the PALFA precursor survey, corresponding to $36^\circ \lesssim \ell \lesssim 50^\circ$. In Section 3, we will compare the performance of the two surveys in this overlap region to make a statement about the efficacy of the PALFA precursor survey.

Data from the PALFA precursor were previously analyzed in Cordes et al. (2006). That analysis used a quasi-real-time QUICKLOOK pulsar search pipeline in which the data were decimated in time and frequency by factors of 8 and 16, respectively, yielding 32 spectral channels and 1024 μs time resolution. Using the decimated data, 11 pulsars were discovered and 29 previously known pulsars were detected. Timing and spectral characteristics from follow-up observations of the newly discovered pulsars are given in Nice et al. (2013).

We have analyzed these same data files at native full time- and frequency-resolution using the PALFA survey's PRESTO 1 pipeline. The full resolution search of the precursor survey data did not yield any pulsar discoveries (and in fact missed some sources flagged by the QUICKLOOK pipeline), but revealed two more previously known normal pulsars (J1946+2611, B1924+16) and the bright MSP B1937+21. The PRESTO 1 zaplist, a list of frequencies and their harmonics related to known sources of radio frequency interference (RFI), may be responsible for this scant improvement over QUICKLOOK results since it was fairly restrictive, "zapping" ∼8% of the spectral region between 0 and 10 Hz (∼84% of known pulsars have spin frequencies in this range). At least one previously known

source, B1925+188, fell inside a zapped portion of the spectrum, but its fourth harmonic was still detectable in PRESTO 1 results. Four other sources that were detected by QUICKLOOK (J1913+1000, B1919+14, J2002+30 and J2009+3326) were not detectable in PRESTO 1 results. Of the 12,488 PALFA precursor beams, 183 (1.5%) were not processed by the PRESTO 1 pipeline, including beams where J1913+1000 and B1919+14 should have been detected. PSRs J2002+30 and J2009+3326 were processed by PRESTO 1 and their spin frequencies were outside zapped portions of the spectrum; why these two sources were not detectable remains unknown, although it is plausible that harmonics of their true spin frequencies could have been "zapped," causing these sources to fall below a detectable threshold.

After the precursor survey was complete, raw data products were decimated to 4-bit resolution and saved in that form. In the process, some files were lost or corrupted (i.e., detection data files for J1913+1000, B1919+14 and B1924+16), so results from Cordes et al. (2006) were used when necessary. We used a complete list of precursor beam positions to determine minimum offset angles from each known source in the survey region, then refolded corresponding 4-bit data files, yielding two additional detections (J1906+0649 and J1924+1631). Table 1 outlines the means by which all sources in the PALFA precursor survey were detected.

2.1. PRESTO 1 Pipeline

The PALFA PRESTO 1 pipeline[22] used to analyze precursor survey data first converted WAPP-format data to SIGPROC filterbank-format (Lorimer 2001). Each filterbank file, one per beam, was then processed independently using various programs from the PRESTO suite of pulsar analysis software[23] (Ransom et al. 2002). Strong narrow-band impulsive and periodic signals were identified as interference by `rfifind`. The filterbank files were then cleaned and reduced-frequency-resolution sub-band files were created at various dispersion measures (DMs). Each group of sub-band files was then used to create time series with DMs close to the DM of the sub-band file. In total 1056 trial DM values were used between $0 \leqslant \mathrm{DM} \leqslant 1003.2$ pc cm^{-3}. The upper limit was chosen to reflect the maximum expected DM in the sky region surveyed (Cordes & Lazio 2003).

Each dedispersed time series was searched for single pulses using `single_pulse_search.py`. Significant pulses ($\sigma > 6$) with widths up to 0.1 s were identified and a diagnostic plot was generated for human inspection. The time series were also Fourier transformed and searched for periodic signals using `accelsearch`. The periodicity search was done in two parts, one for unaccelerated pulsars using up to 16 summed harmonics and the other for accelerated pulsars using up to 8 summed harmonics. The high-acceleration search used a Fourier-domain algorithm (Ransom et al. 2002) with a maximum drift of 50 fast Fourier transform bins. Non-pulsar-like signals were removed from the candidate lists generated from the low and high-acceleration searches. The manicured low and high-acceleration candidate lists were then combined. Candidates harmonically related to a stronger candidate were discarded, while the top 50 candidates with $\sigma > 6$ were "folded" modulo the best Fourier-detected period using `prepfold`, which effectively provides a fully coherent harmonic sum of the signal power. The resulting plots, along with basic metadata about the observations were loaded into a database hosted at Cornell University, where volunteers selected and inspected candidate plots.

2.2. Detection S/N Measurements

For all sources detected by the Quicklook and PRESTO 1 processing pipelines, we refolded data files from beam positions nearest those sources using known pulsar parameters and calculated measured signal-to-noise $(\mathrm{S/N})_{\mathrm{meas}}$ values. For each pulse profile, we used a simple algorithm to determine on- and off-pulse bins, then summed on-pulse intensities and divided by the maximum profile intensity to get an equivalent top-hat pulse width W_{eq} (in bins). Finally, $(\mathrm{S/N})_{\mathrm{meas}}$ is computed with

$$(\mathrm{S/N})_{\mathrm{meas}} = \frac{1}{\sigma_p \sqrt{W_{\mathrm{eq}}}} \sum_{i=1}^{n_{\mathrm{bins}}} (p_i - \bar{p}), \quad (1)$$

as in Lorimer & Kramer (2005), where $\bar{p}$ and σ_p are the mean and standard deviation of off-pulse intensities, respectively, p_i is the intensity of an individual profile bin and each profile had $n_{\mathrm{bins}} = 128$. We divided W_{eq} by the number of bins in a profile n_{bins} to convert to duty cycle δ for each detection. Computed δ and $(\mathrm{S/N})_{\mathrm{meas}}$ values are listed in Table 1.

3. SURVEY RESULTS

To measure the effectiveness of a pulsar survey, we look at the known sources that fall inside the survey region and compare the number of detections to the number of expected detections. Effectiveness will then be evaluated by whether the survey meets/exceeds expectations for detecting individual sources.

3.1. Defining Detectability

The PALFA multibeam receiver is composed of seven beams, each with an average FWHM of $\sim 3\farcm35$; adjacent beams are separated by $\sim 5\farcm5$, or ~ 1.6 half-power beamwidths. Outer beams and the central beam have gains of 8.2 and 10.4 K Jy^{-1} respectively (Cordes et al. 2006). Although previous population studies have modeled gain patterns using Gaussian functions (e.g., Lorimer et al. 2006), we use an Airy disk function to better model the additional gain from the side lobes of individual beams. Although this is not a perfect representation of the PALFA survey's true gain pattern—in fact, the side lobes of the outer ALFA beams are highly asymmetric (see Spitler et al. 2014, for a more precise model)—the Airy disk captures Arecibo's off-axis gain better than the Gaussian model and still provides the simplicity required to run population simulations quickly.

The theoretical signal-to-noise ratio $(\mathrm{S/N})_{\mathrm{th}}$ for a given pulsar with flux density (S_{1400}) measured in mJy at 1400 MHz, spin period P, and pulse width W is given by

$$(\mathrm{S/N})_{\mathrm{th}} = \frac{S_{1400} G \sqrt{n_p t_{\mathrm{obs}} \Delta f}}{\beta T_{\mathrm{sys}}} \sqrt{\frac{1-\delta}{\delta}}, \quad (2)$$

where $\delta = W/P$ is the pulse duty cycle; G is the gain in K Jy^{-1} of a specific beam, $n_p = 2$ is the number of summed polarizations, t_{obs} is the integration time (134 s and 67 s for inner- and outer-Galaxy observations, respectively), $\Delta f = 100$ MHz is the bandwidth, $\beta = 1.16$ is a correction factor that accounts for losses in the digitization process and T_{sys} is the system

[22] Many of the aspects of the PALFA precursor survey data processing described here have since been augmented (e.g., Lazarus 2013), including a new complementary pipeline based on the Einstein@Home distributed volunteer computing platform, e.g., Allen et al. (2013).

[23] https://github.com/scottransom/presto

Table 1
Detections and Expected Detections by the Precursor Survey

PSR Name	P (s)	DM (pc cm^{-3})	ℓ (°)	b (°)	$\Delta\theta$ (′)	Duty Cycle (%)	Flux Density (mJy)	$(S/N)_{th}$	$(S/N)_{meas}$	Pipeline Detected? (QL/P1/Refold)	PALFA Discovery?
J0540+3207	0.524	61	176.7	0.8	1.43	2.1	0.34	62.6	32.8	QL, P1, Refold	Yes
J0628+0909	1.241	88	202.2	–0.9	2.30	1.4	0.06	4.6	21.0	QL, P1, Refold	Yes
J0631+1036	0.288	125	201.2	0.5	1.51	3.3	0.80	85.1	104.1	QL, P1, Refold	
J1855+0307	0.845	402	36.2	0.5	3.24	1.7	0.97	12.4	48.4	QL, P1, Refold	
J1901+0621	0.832	94	39.7	0.8	1.76	5.6	0.47	35.2	21.3	QL, P1, Refold	Yes
B1859+07	0.644	252	40.6	1.1	2.29	3.0	0.90	55.1	38.8	QL, P1, Refold	
J1904+0738	0.209	278	41.2	0.7	0.90	1.9	0.23	54.2	20.1	QL, P1, Refold	Yes
J1904+0800	0.263	438	41.5	0.9	1.99	2.8	0.36	41.0	21.2	QL, P1, Refold	
J1905+0616	0.990	256	40.1	–0.2	1.80	1.5	0.51	69.7	47.4	QL, P1, Refold	
B1903+07	0.648	245	40.9	0.1	0.52	5.6	1.80	266.2	171.3	QL, P1, Refold	
J1905+0902	0.218	433	42.6	1.1	0.50	1.9	0.10	21.1	22.2	QL, P1, Refold	Yes
B1904+06	0.267	472	40.6	–0.3	2.43	5.6	1.70	61.8	104.1	QL, P1, Refold	
J1906+0649	1.287	249	40.7	–0.2	2.53	6.3	0.30	9.2	20.2	Refold	
J1906+0746	0.144	217	41.6	0.1	2.60	1.6	0.55	28.8	15.0	QL, P1, Refold	Yes
J1906+0912	0.775	265	42.8	0.9	2.37	2.5	0.32	19.4	14.4	QL, P1, Refold	
J1907+0740	0.575	332	41.6	–0.1	2.24	2.2	0.41	30.5	25.3	QL, P1, Refold	
J1907+0918	0.226	357	43.0	0.7	3.00	1.6	0.29	7.5	21.8	QL, P1, Refold	
J1908+0734	0.212	11	41.6	–0.3	1.05	3.1	0.54	90.1	23.1	QL, P1, Refold	
J1908+0909	0.337	467	43.0	0.5	1.70	2.2	0.22	28.5	60.9	QL, P1, Refold	
B1907+10	0.284	149	44.8	1.0	1.92	2.3	1.90	206.9	83.8	QL, P1, Refold	
J1910+0714	2.712	124	41.5	–0.9	1.72	1.4	0.36	59.8	15.8	QL, P1, Refold	
B1910+10	0.409	147	44.8	0.2	2.32	3.7	0.22	11.0	...	...	
J1913+1000	0.837	422	44.3	–0.2	1.69	3.8	0.53	66.5	26.0	QL	
J1913+1011	0.036	178	44.5	–0.2	2.69	4.1	0.50	14.1	19.9	QL, P1, Refold	
J1913+1145	0.306	637	45.9	0.5	2.06	4.7	0.43	23.4	...	...	
B1911+11	0.601	100	45.6	0.2	1.90	4.2	0.55	43.9	...	...	
B1913+10	0.405	241	44.7	–0.7	1.51	1.6	1.30	238.2	34.6	QL, P1, Refold	
B1914+13	0.282	237	47.6	0.5	1.78	2.4	1.20	152.8	230.4	QL, P1, Refold	
B1915+13	0.195	94	48.3	0.6	2.29	2.5	1.90	131.6	239.9	QL, P1, Refold	
B1916+14	1.181	27	49.1	0.9	3.04	1.4	1.00	26.9	21.7	QL, P1, Refold	
B1919+14	0.618	91	49.1	0.0	0.45	3.6	0.68	140.2	41.0	QL	
B1921+17	0.547	143	51.7	1.0	3.01	3.6	...	...	46.8	QL, P1, Refold	
J1924+1631	2.935	518	51.4	0.3	0.65	1.0	0.09	35.4	10.5	Refold	
B1924+16	0.580	176	51.9	0.1	0.83	2.5	1.30	363.5	90.9	P1	
B1925+188	0.298	99	53.8	0.9	1.92	5.9	...	...	27.8	QL, P1, Refold	
J1928+1746	0.069	176	52.9	0.1	0.70	5.2	0.28	46.9	29.6	QL, P1, Refold	Yes
B1929+20	0.268	211	55.6	0.6	3.78	2.0	1.20	1.7	24.0	QL, P1, Refold	
B1937+21	0.00156	71	57.5	–0.3	2.41	14.9	13.20	327.0	180.5	P1, Refold	
J1946+2611	0.435	165	62.3	0.6	2.61	2.4	...	...	18.5	P1, Refold	
B1952+29	0.427	7	66	0.8	2.53	4.5	8.00	325.8	117.3	QL, P1, Refold	
J1957+2831	0.308	138	65.5	–0.2	1.57	3.6	1.00	131.2	30.0	QL, P1, Refold	
J2002+30	0.422	196.0	67.9	–0.2	1.21	3.7	...	...	60.7	QL, Refold	
B2000+32	0.697	142	69.3	0.9	2.16	1.8	1.20	121.7	49.1	QL, P1, Refold	
B2002+31	2.111	234	69.0	0.0	3.30	1.3	1.80	26.3	94.4	QL, P1, Refold	
J2009+3326	1.438	263	71.1	0.1	0.82	3.0	0.15	32.4	23.9	QL, Refold	Yes
J2010+3230	1.442	371	70.4	–0.5	0.60	2.2	0.12	32.6	23.4	QL, P1, Refold	Yes
J2011+3331	0.932	298	71.3	–0.0	2.50	2.6	0.38	21.2	39.4	QL, P1, Refold	Yes
J2018+3431	0.388	222	73.0	–0.8	1.70	2.0	0.24	47.4	31.7	QL, P1, Refold	Yes

Notes. A comprehensive list of all pulsars detected by the precursor survey as well as those we expected to detect, given their high $(S/N)_{th}$ quantities. We list each pulsar's period (P), dispersion measure (DM), Galactic longitude (ℓ), Galactic latitude (b), angular offset from the closest beam ($\Delta\theta$) and duty cycle (δ), as well as $(S/N)_{th}$, $(S/N)_{meas}$. PALFA precursor data were run through two processing pipelines, Quicklook and PRESTO 1 (described in Section 2), then converted into 4-bit files and stored. Pulsars detected by Quicklook (QL) or PRESTO 1 (P1) pipelines are marked accordingly; those detected after refolding archived, 4-bit data files have "Refold" in the "Pipeline Detected?" column. Previously unknown pulsars discovered by the precursor survey are marked with a "Yes" in the last column. For sources without an available flux density measurement, we did not compute $(S/N)_{th}$. Previously determined parameters (P, DM, ℓ, b and flux density) were obtained from the ATNF Pulsar Catalog (Manchester et al. 2005). Missing parameters, $(S/N)_{th}$ and $(S/N)_{meas}$, for example, are denoted by dashes (—).

temperature measured in K (Dewey et al. 1985). Flux densities S_{1400} were obtained from the ATNF Pulsar Catalog (Manchester et al. 2005) for known pulsars and Nice et al. (2013) for pulsars discovered by the PALFA precursor survey. Equation (2) is an approximation since this treatment assumes top-hat pulse profiles and ignores the considerable variability in pulse shape. The majority of pulsars have Gaussian-shaped profiles, however, so this approximation works well in most cases.

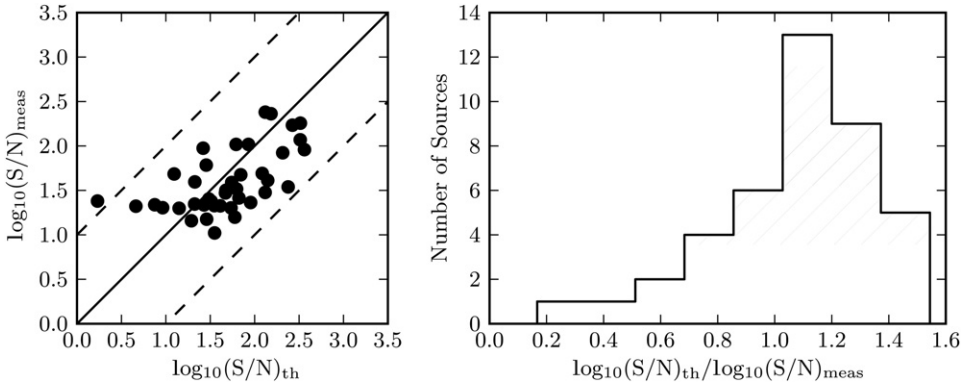

Figure 1. Left plot shows theoretical vs. measured S/Ns for each source with both quantities available. If the two values match for a given source, the data point for that source should lie along the solid line with slope unity. The loose correlation shown here is a result of a combination of effects, but most notably, there can be as much as ∼30% fractional error in $(S/N)_{th}$ due to uncertainties in initial flux measurements, which were taken from the ATNF Pulsar Catalog (Manchester et al. 2005); interstellar scintillation and RFI also contribute to the large scatter. Dashed lines give a reference for sources whose theoretical and measured S/N values are different by a factor of 10. The right plot emphasizes the fact that, in addition to the significant dispersion, $(S/N)_{meas}$ is smaller than $(S/N)_{th}$ in many cases. This systematic offset implies a poor understanding of the noise environment and suggests that the maximum sensitivity limits of the survey have not yet been realized.

Hereafter $(S/N)_{th}$ will refer to theoretical signal-to-noise ratios, computed using Equation (2), while $(S/N)_{meas}$ refers to signal-to-noise ratios measured from PALFA detections as described in Section 2.2 and specifically Equation (1).

Since gain is a function of a source's angular offset from the beam center, we model it as an Airy disk so that the gain

$$G = G_0\left(\frac{2J_1(ka\sin(\theta))}{ka\sin(\theta)}\right)^2, \quad (3)$$

where J_1 is a Bessel function of the first kind, G_0 is the maximum on-axis gain of the beam, $k = 2\pi/\lambda$ is the wavenumber (λ, the observation wavelength), a is the effective aperture radius (∼220 m), and θ is the angular offset of a source from the beam center, measured in radians. In predicting S/N for a given pulsar, the pulsed nature of its emission must be taken into account, as shown by the final term in Equation (2). For all pulsars that were detected in the precursor survey, we computed W_{eq}, then δ as described in Section 2.2. For sources that were not detected, we divide the pulse width at half maximum (W50), from the ATNF Pulsar Catalog (Manchester et al. 2005), by the period to compute δ, then $(S/N)_{th}$. Finally, T_{sys} includes the receiver temperature ($T_{rec} = 24$ K) and sky temperature (T_{sky}), which varies as a function of position and frequency as shown by Haslam et al. (1982). Since this sky temperature map describes T_{sky} at 408 MHz, we convert these values into 1.4 GHz sky temperatures using an assumed spectral index of $\alpha = 2.6$, that is $T_{sky} \propto \nu^{-\alpha}$.

Although there are many factors involved, we assume a 1:1 relationship between $(S/N)_{meas}$ and $(S/N)_{th}$ in order to use S/N as a prediction tool for the detectability of known sources. The true relationship between $(S/N)_{meas}$ and $(S/N)_{th}$ can be seen in Figure 1.

Using a complete list of beam positions, we found the survey observations carried out closest to known pulsars in the precursor region (i.e., minimizing angular offset, θ). For each of these positions, we found the maximum expected gain for a given pulsar using Equation (3). Previously measured parameters for known pulsars allowed us to compute a theoretical signal-to-noise, $(S/N)_{th}$, as shown in Equation (2). We define a known pulsar to be detectable if we find $(S/N)_{th} > 9$ for that pulsar. A full list of pulsars detected by the precursor survey as well as those considered detectable due to their $(S/N)_{th}$ values can be found in Table 1. Before PALFA began, there were 84 known pulsars positioned inside the target precursor survey region, although this sky area was not covered uniformly; 31 of 84 were deemed detectable, while 33 were actually detected, and seven had no previous flux measurements. Of the 51 non-detections, most can be attributed simply to the sources not being close to a PALFA precursor survey beam pointing, as the survey had only limited coverage in this region. Figure 2 shows the portion of the precursor survey that overlaps with the PMPS), an example of this limited coverage. Three of the 51 non-detections (B1910+10, J1913+1145, and B1911+11) were unexpected, since $(S/N)_{th} > 9$ for these sources; one of the 33 detections (B1929+20) was also unexpected, given its low $(S/N)_{th}$ value. The non-detections could be due to a variety of factors—most likely RFI. Scintillation could have also suppressed the expected signal during precursor survey observations or boosted the signal during initial flux measurements. It is unlikely scintillation affected the detectability of J1913+1145, however, because of this source's high DM (637 pc cm^{-3}). Given the short integration time near each of these sources (134 s), the pulse-to-pulse variability may have strongly affected $(S/N)_{meas}$ since relatively few pulses were recorded. Also, because of the

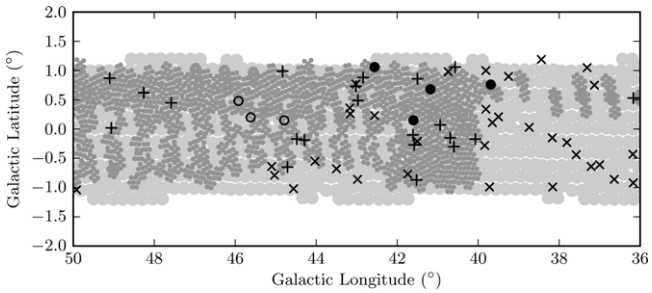

Figure 2. Beam positions for the PMPS (light gray) and PALFA precursor survey (dark gray) are shown here with known pulsar positions superimposed. The Parkes beam radii are about four times as large as those of Arecibo; the points indicating beam positions have been scaled appropriately relative to one another. Only PMPS beams within 1.°2 of the Galactic plane are plotted since this more than covers the Galactic latitude limits of the PALFA precursor survey. Of the 58 previously known pulsars plotted here, many were too far from the nearest precursor survey beam center, making them undetectable (denoted by ×). Only 24 of 59 were deemed detectable, given the precursor survey's patchy coverage of this Galactic sector, and were considered in comparing the two surveys. Known pulsars detected by the precursor survey are marked with +, while expected detections that were missed are marked with ◯s. Filled circles indicate the positions of PALFA precursor survey discoveries in the region overlapping with PMPS.

large error bars on $(S/N)_{th}$ (∼30% fractional error) due to uncertainties in flux measurements, the sources may simply be weaker than expected.

Although most sources with high $(S/N)_{th}$ values were detected by the precursor survey's processing pipelines, five such sources were not. For each of these cases, we employed the same procedure as introduced in Section 2.2, using known periods and dispersion measures to dedisperse and fold the data from the closest pointing to each source. For the three sources mentioned earlier (B1910+10, B1911+11, and J1913+1145), no pulsations were detected; for the other two, J1906+0649 and J1924+1631, pulsations are evident, but relatively weak. PSR J1906+0649 was likely missed because of the RFI environment at Arecibo.

In addition to the 33 re-detected pulsars in the region, PSR J1924+1631 was discovered shortly after the precursor survey was completed, when the PALFA survey underwent an upgrade to a new backend with three times more bandwidth. This source was then retroactively found in precursor survey data with $(S/N)_{meas}$ just above the detection threshold and has therefore been included in analysis that follows. Strong RFI present in the refolded precursor data explains why this source was not discovered earlier. P. Lazarus (2014, in preparation) will describe the most recent processing pipeline in detail, address the RFI environment and its effect on the PALFA survey's "true" sensitivity.

4. PMPS OVERLAP REGION

The PALFA precursor survey region overlaps the region covered by the PMPS in Galactic longitude, $36^\circ \lesssim \ell \lesssim 50^\circ$. Although there were 58 previously known pulsars in this longitude range and within ∼1° of the Galactic plane when the precursor survey took place (see Figure 2), we compare the PMPS and precursor survey detections only based on sources deemed detectable by the precursor survey. We justify this criterion based on the fact that, due to patchy coverage, only ∼10% of the overlap region lies within an angular offset $\Delta\theta \sim 1.'2$ of a precursor beam center. We choose $1.'2$ since this is the average angular offset $\langle\Delta\theta\rangle = \mathrm{FWHM}/2\sqrt{2}$ for the precursor survey. Half of all sources that fall within a radius $R = \mathrm{FWHM}/2$ of the nearest beam center will also be within the average angular offset $\langle\Delta\theta\rangle$.

The PMPS discovered or detected all 24 of the previously known pulsars in this region considered detectable by the PALFA precursor survey. The precursor survey detected 21 of these, and discovered an additional four sources in this region. The PMPS retroactively detected two of these four precursor discoveries in archival data (e.g., Lorimer et al. 2006).

One of the three detectable known pulsars that the precursor survey missed, B1910+10, had a $(S/N)_{th}$ value of ∼11 (see Table 1), just above the detectability threshold of $(S/N)_{th} = 9$; the other two, J1913+1145 and B1911+11, were expected to be detected with $(S/N)_{th} = 23$ and 36, respectively. Error in $(S/N)_{th}$ is ∼30%, which reflects the error in flux measurements and can easily explain the first non-detection. It is much harder to explain why J1913+1145 and B1911+11 were not detected, given their high $(S/N)_{th}$ values, but other systematics such as RFI and scintillation may explain these discrepancies.

The four precursor survey discoveries—J1901+0621, J1904+0738, J1905+0902 and J1906+0746—have relatively high dispersion measures and were all detected near the signal-to-noise threshold with $15 < (S/N)_{meas} < 22$, so it is not surprising that they were not detected by previous surveys. PSR J1906+0746 is a 144 ms pulsar in a relativistic, 3.98 hr orbit and was initially missed during manual inspection of PMPS candidate plots due to RFI with a period similar to that of the pulsar (Lorimer et al. 2006). Both J1906+0746 and J1901+0621 were found retroactively in Parkes data, which was expected, given that both are moderately bright sources with flux densities at 1400 MHz of about 0.5 mJy. The other two discoveries, J1904+0738 and J1905+0902, are much fainter—0.23 and 0.097 mJy, respectively (Nice et al. 2013). These discoveries show preliminary evidence that with Arecibo's high sensitivity, the PALFA precursor survey probed a deeper and lower-luminosity pulsar population than previous surveys. However, the three unexpected non-detections suggest that the PALFA precursor survey did not realize its full sensitivity and more work is required to better understand Arecibo's RFI environment and develop mitigation techniques.

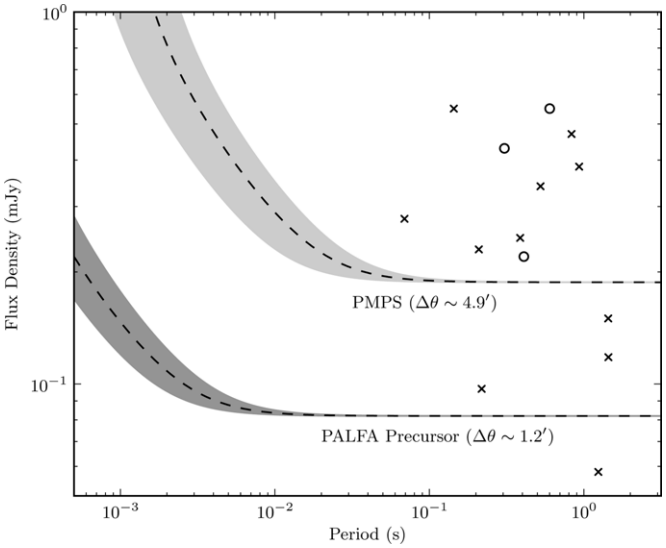

Figure 3. Sensitivity as a function of period for the precursor survey is shown in dark gray; the PMPS curve (light gray) is shown here for comparison. The dashed lines in each case show the sensitivity to DM = 100 pc cm^{-3} sources, while upper and lower limits of the shaded regions give minimum flux density sensitivity to pulsars with DM = 150 or 50 pc cm^{-3}, respectively. These curves are plotted using the average angular offset $\langle\Delta\theta\rangle$between a source and a beam position. For a random distribution of pulsars on the sky, ∼50% should fall within an angle $\langle\Delta\theta\rangle$from the nearest beam position. Precursor survey discoveries are superimposed as ×, while expected detections B1910+10, B1911+11 and J1913+1145 that were missed by the PALFA precursor survey, but detected by PMPS are shows with ◯.

The relative sensitivity limits as a function of period and DM for the PMPS and precursor surveys are compared in Figure 3. To generate these curves, we used an average T_{sky} value for each survey region, assumed a constant pulse duty cycle of $\delta = 0.05$, and applied the empirical pulse broadening function from Bhat et al. (2004) to account for multipath scattering in the interstellar medium. For the three objects that were detected at Parkes, but not in the PALFA precursor survey (B1910+10, J1913+1145 and B1911+11), all have periods between 300 and 600 ms, a regime where the PMPS nominal sensitivity limit in Figure 3 is about twice as high as the precursor survey's. However, the angular offsets to these sources ($6.'6$, $4.'7$ and $2.'5$, respectively, for PMPS and precursor values can be found in Table 1) imply that both surveys were equally sensitive to them since the PALFA precursor beam (FWHM ∼ $3.'35$) is much narrower than that of the PMPS (FWHM ∼ $14.'4$) and its sensitivity therefore drops off more quickly as a function of $\Delta\theta$. Taking angular

offsets into account, B1910+10 ($S_{1400} = 0.22$ mJy) falls below the adjusted minimum sensitivity limit (∼0.26 mJy for both surveys), but B1911+11 and J1913+1145 do not, so angular offsets alone do not explain why these sources went undetected. Since other sources with lower flux densities and similar angular offsets *were* detected (i.e., J0628+0909, J1906+0649, J1906+0912, J1907+0740, J1907+0918, J2011+3331), we conclude that transient effects such as RFI decreased the signal-to-noise ratios of B1910+10, B1911+11 and J1913+1145 and possibly scintillation for the former two.

5. POPULATION ANALYSIS

The analysis presented here uses PsrPopPy—a package that models the Galactic population and evolution of pulsars. With this software, we populated a synthetic galaxy with pulsars whose attributes like cylindrical spatial coordinates, period, DM, luminosity, etc. were chosen from pre-determined PDFs (Lorimer et al. 2006). PsrPopPy[24] is a Python implementation of PSRPOP,[25] which was written in Fortran (Lorimer et al. 2011); it shares much of the same functionality, but the object-oriented nature of Python and improved modularity of the code make it more readable and easier to write plug-ins for specific modeling purposes. Further details on the PsrPopPy software package are forthcoming (Bates et al. 2014).

5.1. Generating Pulsar Population PDFs

In order to deduce the sizes of the underlying Galactic normal and millisecond pulsar populations, we compared the results of PsrPopPy simulations to the PALFA precursor survey's detection statistics for each of these two classes of pulsar. In each case, we made a set of assumptions about the underlying population (see Table 2) and drew spatial and intrinsic pulsar parameters from assumed distributions to form a synthetic Galactic population. We simulated a survey of this synthetic population by computing $(S/N)_{th}$ as was discussed in Section 3. Again, detections were then defined as sources with $(S/N)_{th} > 9$. The assumptions that went into our simulations, outlined in Table 2, were largely drawn from the work by Lorimer et al. (2006) for the normal pulsar population. In that paper, however, the luminosity distribution for normal pulsars was assumed to behave as a power law with a low-luminosity cutoff of 0.1 mJy kpc^2. Since the PALFA precursor survey's sensitivity dips below this cutoff value in some cases, we instead adopt a log-normal luminosity distribution, introduced by Faucher-Giguère & Kaspi (2006).

Since far fewer MSPs are known, we have very little information about the population's spatial and intrinsic parameter distributions, so some assumptions are simply adopted from the normal pulsar population (luminosity and radial distributions), while others are grounded in some preliminary experimental results (scale height, period, and duty cycle distributions). In this case, we used a Gaussian radial distribution with a standard deviation of 6.5 kpc and an exponential scale height larger than that of normal pulsars to reflect the fact that MSPs are distributed more uniformly across the sky. The Gaussian radial model for MSPs in the Galaxy is similar to that of normal pulsars, but makes no assumption about a deficiency of sources toward the Galactic center, an effect observed from full *normal* pulsar population synthesis and modeled with a Gamma function (Lorimer et al. 2006).

[24] https://github.com/samb8s/PsrPopPy
[25] http://psrpop.sourceforge.net/

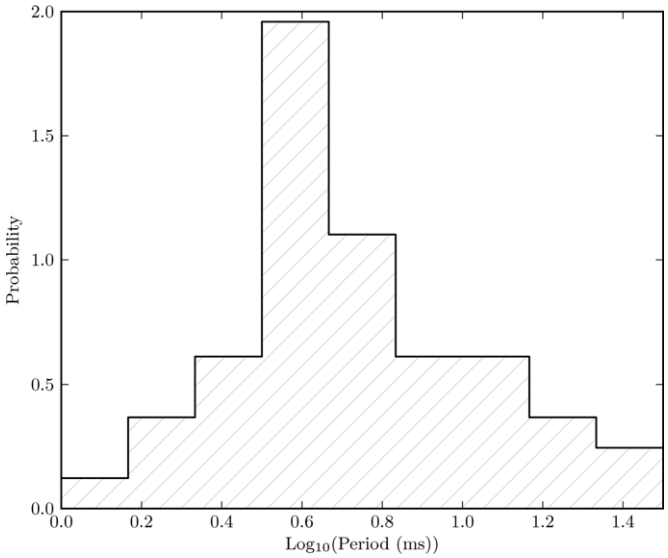

Figure 4. This histogram shows the ad-hoc MSP period distribution used in simulations, which peaks at periods close to 3 ms. A more precise, empirically based distribution is forthcoming and will be based on MSPs detected in the PMPS and HTRU surveys.

We adopted the period distribution shown in Figure 4 from Lorimer (2013), where it was initially realized by adjusting the weights of various bins from a flat distribution (in log P) until preliminary simulations matched the sample of observed MSPs from PMPS. Unlike normal pulsar duty cycles, which show inverse proportionality to the square root of spin period (i.e., shorter-period pulsars have wider pulses), MSPs tend to exhibit relatively constant duty cycle across period, with larger scatter about some mean value than the normal pulsar population (Kramer et al. 1998; Smits et al. 2009). Therefore, our simulations assumed MSP duty cycles to be independent of period.

To make the simulated detections as realistic as possible, we used precursor survey parameters in signal-to-noise ratio calculations, and modified PsrPopPy to accept the survey's true pointing positions, as well as corresponding integration times and specific beam gain values. For each population class, we performed simulated precursor surveys across a range of trial population sizes (85,000–130,000 for normal pulsars and 5000–50,000 for MSPs). For each trial, we performed 2000 simulated realizations of independent Galactic populations for MSPs and normal pulsars respectively. To form a likelihood function describing pulsar population size, we compared the results of these simulations to the true number of detections for each population class in the precursor survey. The precursor survey only detected a single MSP (B1937+21), so the likelihood was computed by dividing the number of simulations that resulted in a single detection by the total number of simulations at that population size.

Of the 45 detections listed in Table 1, we exclude B1937+21 (MSP) from our normal pulsar analysis. Although J1906+0746 is in a binary system, it is a young pulsar with a characteristic age of 112 kyr and has likely not undergone recycling from its companion, so we include it in our analysis. The likelihood function was formed by dividing the number of simulations that detected 44 pulsars by the total number of simulations at a given trial population size. We fit binomial distributions to simulated likelihood functions for normal and MSP populations (shown in Figure 5) in order to smooth simulation results and

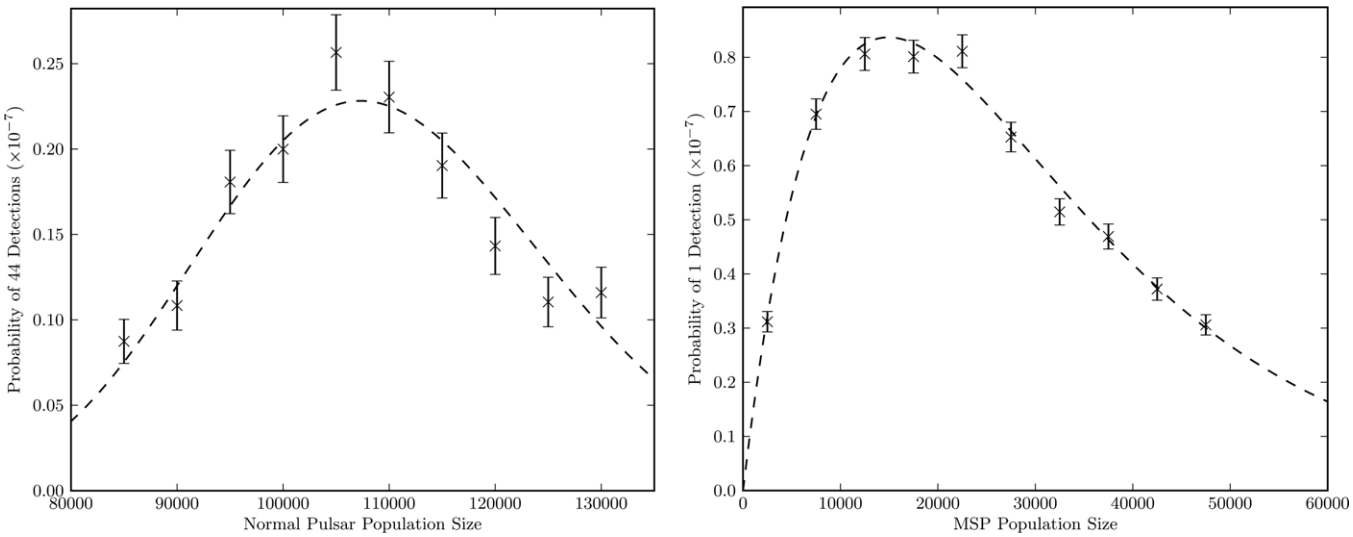

Figure 5. In each plot, black × show results of 2000 population simulations at 10 different trial pulsar population sizes. The normal pulsar population PDF (left plot) was constructed with trial simulations using population sizes between 85,000 and 130,000 sources, while the MSP PDF (right plot) used between 5000 and 50,000 sources in trial simulations. In both cases the black dashed line shows a normalized binomial distribution fit to the data. Using these fits, we find that the most probable *detectable* Galactic normal and millisecond pulsar population sizes are ∼107,000 and ∼15,000, respectively.

Table 2
Parameters Used in Population Simulations

Prior Distribution Parameter	Normal PSR Simulations	MSP Simulations
Luminosity	Log Normal: $\mu = -1.1; \sigma = 0.9$	Log Normal: $\mu = -1.1; \sigma = 0.9$
Period	Log Normal: $\mu = 2.7, \sigma = -0.34$	(see Figure 4)
Radial	Gamma Function: (see Lorimer et al. 2006)	Gaussian: $\sigma = 6.5$ kpc
Scale height	0.33 kpc	0.5 kpc
Duty Cycle	(explained in Section 5.1)	(explained in Section 5.1)
Electron Model	NE2001	NE2001

Notes. Assumed parameter values/distributions for normal and millisecond pulsar populations respectively. These parameters are used as input values to the appropriate PsrPopPy functions, which generate an underlying, synthetic population. Changing input parameters directly affects the number of detections expected from a given simulated survey.

provide integrable functions to determine confidence intervals. For an underlying population of size N, a given simulation has n successes (detections) and $N-n$ failures (non-detections); these kinds of binary outcomes are nicely modeled by binomial distributions.

The binomial distributions provide the functional form

$$p(n|N,\theta) = \frac{N!}{n!(N-n)!}\theta^n(1-\theta)^{N-n}, \quad (4)$$

which describes the probability of drawing n pulsars from a total population of N given some detection probability θ. To select the θ value that produces posterior PDFs that best match the simulated data, we chose the one that minimized χ^2, computed by comparing simulated to expected population distributions. Finally, the posterior population size PDFs are normalized so that they could be used to quote confidence intervals. With some number $n_{\rm success}$ of successful realizations (simulations in which the target number of detections is reached), the Poissonian error is given by $\sqrt{n_{\rm success}}$. Data points that reflect the probability of detecting exactly the target number of pulsars at a trial population size and their error bars are multiplied by the same constant required to normalize the best fit PDF. After looking at multiple realizations of the simulated data presented in Figure 5 and comparing the standard deviation of data points at each population size to assumed Poissonian error bar magnitudes, we determined that the Poisson model accurately reflects the uncertainties in population sizes.

By integrating the PDFs shown in Figure 5, we find the mode and 95% confidence interval for the normal pulsar population size to be $107{,}000^{+36{,}000}_{-25{,}000}$. We find a lower mode for the MSP population size, $15{,}000^{+85{,}000}_{-6000}$ and the high uncertainty in the corresponding 95% confidence interval reflects the fact that our prediction depends on a single MSP detection in the precursor survey. These results describe the respective Galactic pulsar populations that are beaming toward Earth and errors on most likely population sizes account only for statistical uncertainties due to the limited number of detections in the PALFA precursor survey, not for other sources (e.g., uncertainties in scale height, luminosity distribution, electron density model, etc.).

The confidence interval that the precursor survey places on the normal pulsar population is consistent with earlier results; Faucher-Giguère & Kaspi (2006) predict 120,000 ± 20,000 detectable normal pulsars, also using a log-normal distribution to model the pulsar luminosity function. The predicted MSP population size is also consistent with previous estimates; the upper limit we find easily encompasses the population size prediction made by Levin et al. (2013), although the lower limit quoted in that paper, 30,000 ± 7000, is more constraining. Neither of these 95% confidence intervals is tight enough to put strict constraints on normal or millisecond pulsar population

sizes, but the consistency is encouraging and we expect the full PALFA survey to place much more stringent constraints on these populations when complete.

6. RESULTS AND DISCUSSION

Using input parameters from Table 2 to generate a synthetic, Galactic normal pulsar population, we found that the PALFA precursor survey should be expected to detect ∼40 sources. Through periodicity searches, 43 were found, which indicates that current population parameters, initially determined using PMPS results, are already quite accurate and applicable to a variety of situations. As we mentioned in Section 3.1, three sources that we expected to detect were not detected, but it is common for $(S/N)_{th}$ and $(S/N)_{meas}$ values to not match perfectly. Due to uncertainties in initial flux measurements, there can be as much as ∼30% fractional error in $(S/N)_{th}$. Referring again to Figure 1, we show a general trend toward a slope of unity when plotting theoretical versus measured S/N for the detections made by the precursor survey, but there is significant scatter in these comparisons. Scatter like this can be caused by scintillation, RFI, poor prior flux measurements or some combination of all of these.

The precursor survey discovered 11 pulsars, 4 of which fell inside the region overlapping PMPS, allowing us to directly compare their respective sensitivities. While PMPS detected almost three times as many sources in this region, this discrepancy was largely due to the differences in sky coverage—PMPS covered this area uniformly, while the precursor survey had large blocks of coverage missing and slight gaps between pointings due to a "sparse sampling" technique. In fact, only ∼25% of the overlap region was covered by the precursor survey to a sensitivity greater than or equal to that of PMPS. Even so, the PALFA precursor survey discovered four pulsars that PMPS missed; two of these four were retroactively found by reanalyzing archival data but the others(J1904+0738 and J1905+0902) have high dispersion measures and very low fluxes—an encouraging, albeit small, piece of evidence that Arecibo's sensitivity gives PALFA a glimpse at fainter and more distant pulsars. Figure 3 in Nice et al. (2013) uses more recent PALFA discoveries to show further evidence of PALFA probing deeper than previous surveys as do recent discoveries mentioned in Crawford et al. (2012).

We simulated a range of Galactic pulsar populations—both non-recycled and recycled—of various sizes and used the PALFA precursor survey's detection statistics to place limits on normal and millisecond pulsar population sizes respectively. By comparing experimental results to simulations, we formed PDFs for normal and MSP population sizes, then integrated these PDFs to define confidence intervals.

Assuming the most probable normal and millisecond population sizes according to the simulations described in Section 5.1 are correct, we ran 1000 trials with the same distribution parameter assumptions for each population to determine the most likely number of detections by the beginning of 2014 and after PALFA is complete. Averaging the results of these 1000 trials in each case, we determine a predicted number of detections, then quote errors that are directly proportional to the 95% confidence limits from normal and millisecond pulsar population PDFs. Following this procedure, we expect the full PALFA survey to detect 1000^{+330}_{-230} normal pulsars (this includes previously known sources that are re-detected) and 30^{+200}_{-20} MSPs. Identical estimation techniques predict that 490^{+160}_{-115} normal pulsars and 12^{+70}_{-5} MSPs should have been detected by the beginning of 2014, but at the time, PALFA had detected 283 normal pulsars and 31 MSPs, respectively.[26]

The discrepancy between observed and predicted detection rates is notable for the normal pulsar population. Given the numbers quoted here, PALFA has currently detected just over 50% of the expected number of normal pulsars, according to simulations. These simulations do not yet take into account the local RFI environment of the PALFA survey, which certainly plays a role in the perceived dearth of pulsar detections as of early 2014. Two pulsars that went undetected by both QUICKLOOK and PRESTO 1 pipelines in the precursor survey, J1906+0649 and J1924+1631, provide evidence that initial processing techniques were not optimal and improvements are necessary. In repeated simulations of precursor detections in the inner Galaxy region, we find 30–50% of simulated, detectable sources had S/N values between 9 and 15 (just above the detection threshold). In the precursor survey, only about 10% of detections had $(S/N)_{meas}$ values in this regime. Although the precursor survey discovered mostly low flux density sources, the fact that only a small fraction of detections were near the S/N threshold suggests that some sources were missed or assumptions that determine our sensitivity curves are not entirely correct.

A potential factor of two lower sensitivity to normal pulsars because of RFI would bring the survey yield and simulated population into agreement. The most recent PALFA survey pipeline will be described in depth by P. Lazarus (2014, in preparation) and that paper will also construct PALFA's "true" sensitivity curve, taking into account the RFI environment by injecting artificial signals of varying strength into real data. In future work, we will reprocess precursor survey data with the current pipeline to see if it improves the shortcomings of earlier versions (e.g., inconsistent detection statistics, noted in Table 1).

The assumed radial distribution of pulsars in the Galaxy (see Table 2) could also contribute to the discrepancy between expected (simulated) and true pulsar yields. Since the distribution is based on extrapolated results from the PMPS, which surveyed higher-populated regions of the sky, population density estimates for longitudes farther from Galactic center may be inaccurate. Overestimated pulsar population densities in the Galactic longitude range surveyed by the PALFA precursor survey could be a factor in the discrepancies we find between expected and actual pulsar detections there. Future refinement of pulsar population models using PALFA results will provide consistency checks for existing population model parameters.

We note that the current number of MSPs detected by PALFA is consistent with predictions, but this is not surprising, given the high uncertainties in our model due to the precursor survey only detecting one MSP. As the number of detections increases, future predictions will be far more constraining so that we can re-examine initial assumptions about the MSP population characteristics.

Future population studies with the complete PALFA survey will contribute substantially to current population models because of the Galactic longitude ranges covered and Arecibo's unrivaled sensitivity (especially in the millisecond pulse period regime). As the number of normal and millisecond pulsar detections increases, our ability to refine specific, simulated model parameters that describe each underlying population will improve significantly.

[26] See http://www.naic.edu/∼palfa/newpulsars for discoveries; re-detected sources are as yet unpublished.

The Arecibo Observatory is operated by SRI International under a cooperative agreement with the National Science Foundation (AST–1100968), and in alliance with Ana G. Méndez-Universidad Metropolitana, and the Universities Space Research Association. M.A.M. and J.K.S. are supported through NSF PIRE award 0968296. D.J.N. is supported through NSF grant 0647820. V.M.K. was supported by an NSERC Discovery and Accelerator Grant, the Canadian Institute for Advanced Research, a Canada Research Chair, Fonds de Recherche Nature et Technologies, and the Lorne Trottier Chair in Astrophysics. J.W.T.H. acknowledges funding from NWO and ERC. Work at Cornell was supported by NSF Grants 0507747 and 1104617 and made use of the Cornell Center for Advanced Computing. Pulsar research at UBC is supported by an NSERC Discovery Grant and Discovery Accelerator Supplement and by the Canada Foundation for Innovation. P.L. acknowledges support of IMPRS Bonn/Cologne and NSERC PGS–D.

REFERENCES

Allen, B., Knispel, B., Cordes, J. M., et al. 2013, ApJ, 773, 91
Bates, S. D., Bailes, M., Bhat, N. D. R., et al. 2011, MNRAS, 416, 2455
Bates, S. D., Lorimer, D. R., Rane, A., & Swiggum, J. 2014, MNRAS, 439, 2893
Bhat, N. D. R., Cordes, J. M., Camilo, F., Nice, D. J., & Lorimer, D. R. 2004, ApJ, 605, 759
Burgay, M., Bailes, M., Bates, S. D., et al. 2013, MNRAS, 433, 259
Cordes, J. M., & Chernoff, D. F. 1997, ApJ, 482, 971
Cordes, J. M., Freire, P. C. C., Lorimer, D. R., et al. 2006, ApJ, 637, 446
Cordes, J. M., & Lazio, T. J. W. 2003, arXiv:astro-ph/0301598
Crawford, F., Stovall, K., Lyne, A. G., et al. 2012, ApJ, 757, 90
Demorest, P. B., Ferdman, R. D., Gonzalez, M. E., et al. 2013, ApJ, 762, 94
Dewey, R. J., Taylor, J. H., Weisberg, J. M., & Stokes, G. H. 1985, ApJL, 294, L25
Dowd, A., Sisk, W., & Hagen, J. 2000, IAU Colloq. 177: Pulsar Astronomy—2000 and Beyond (San Francisco, CA: ASP), 202, 275
Faucher-Giguère, C.-A., & Kaspi, V. M. 2006, ApJ, 643, 332
Faulkner, A. J., Stairs, I. H., Kramer, M., et al. 2004, MNRAS, 355, 147
Haslam, G., Wielebinski, R., & Priester, W. 1982, S&T, 63, 230
Hobbs, G., Faulkner, A., Stairs, I. H., et al. 2004, MNRAS, 352, 1439
Keith, M. J., Jameson, A., van Straten, W., et al. 2010, MNRAS, 409, 619
Kramer, M., Bell, J. F., Manchester, R. N., et al. 2003, MNRAS, 342, 1299
Kramer, M., Xilouris, K. M., Lorimer, D. R., et al. 1998, ApJ, 501, 270
Lazarus, P. 2013, in IAU Symp. 291, Neutron Stars and Pulsars: Challenges and Opportunities After 80 Years, ed. T. Montmerle, 35
Levin, L., Bailes, M., Barsdell, B. R., et al. 2013, MNRAS, 434, 1387
Lorimer, D. 2011, ascl soft, 7019
Lorimer, D. R. 2001, LRR, 4, 5
Lorimer, D. R. 2005, LRR, 8, 7
Lorimer, D. R. 2010, HiA, 15, 807
Lorimer, D. R. 2013, in IAU Symp. 291, Neutron Stars and Pulsars: Challenges and Opportunities After 80 Years, ed. T. Montmerle, 237
Lorimer, D. R., Bailes, M., Dewey, R. J., & Harrison, P. A. 1993, MNRAS, 263, 403
Lorimer, D. R., Faulkner, A. J., Lyne, A. G., et al. 2006, MNRAS, 372, 777
Lorimer, D. R., & Kramer, M. 2005, Handbook of Pulsar Astronomy (Cambridge: Cambridge Univ. Press)
Lorimer, D. R., Stairs, I. H., Freire, P. C., et al. 2006, ApJ, 640, 428
Manchester, R. N., Hobbs, G. B., Teoh, A., & Hobbs, M. 2005, yCat, 7245, 0
Manchester, R. N., Lyne, A. G., Camilo, F., et al. 2001, MNRAS, 328, 17
Mickaliger, M. B., Lorimer, D. R., Boyles, J., et al. 2012, ApJ, 759, 127
Morris, D. J., Hobbs, G., Lyne, A. G., et al. 2002, MNRAS, 335, 275
Nice, D. J., Altiere, E., Bogdanov, S., et al. 2013, ApJ, 772, 50
Ransom, S. M., Eikenberry, S. S., & Middleditch, J. 2002, AJ, 124, 1788
Siemens, X., Ellis, J., Jenet, F., & Romano, J. D. 2013, CQGra, 30, 224015
Smits, R., Lorimer, D. R., Kramer, M., et al. 2009, A&A, 505, 919
Spitler, L. G., Cordes, J. M., Hessels, J. W. T., et al. 2014, ApJ, submitted (arXiv:1404.2934)
Vivekanand, M., & Narayan, R. 1981, JApA, 2, 315